Med Chem Res (2013) 22:2196–2206
DOI 10.1007/s00044-012-0212-x

MEDICINAL CHEMISTRY RESEARCH

ORIGINAL RESEARCH

Synthesis and insect antifeedant activity of stilbene derivatives against *Brontispa longissima* Larvae

Ying-Qian Liu · Xiao-Jing Li · Chun-Yan Zhao · Yan Lu · Wen-Qun Li · Zhen-Ling Liu · Gang Feng · Liu Yang

Received: 9 April 2011 / Accepted: 20 August 2012 / Published online: 6 September 2012

Abstract Continuing our search for natural product-based compounds for the control of *B. longissima* Larvae, 25 stilbene analogs were synthesized and evaluated for insect antifeedant activity against third-instar larvae of *B. longissima* for the first time. Among all the tested compounds, especially compounds **3a**, **3c**, and **6** showed pronounced antifeedant activities with AFC_{50} values of 0.218, 0.327, and 0.226 mg/mL, respectively. The different antifeedant activity ranges of these compounds indicated that variation of chemical structures in the stilbene skeleton markedly affected the activity profiles of this compound class, and some important SAR information has been revealed from it. In addition, to understand the structural requirements for antifeedant activities of the 25 synthesized stilbene analogs, a comparative molecular field analysis (CoMFA) model, which yielded the leave-one-out (LOO) cross-validated correlation coefficient (q^2) of 0.533 and a non-cross-validated correlation coefficient (r^2) of 0.929, was constructed. Together, these preliminary results may be useful in guiding further modification of stilbenes in the development of potential new antifeedants.

Keywords Stilbenes · insect antifeedants · *Brontispa longissima* · CoMFA · 3D-QSAR study

Y.-Q. Liu (✉) · X.-J. Li · C.-Y. Zhao · Y. Lu · W.-Q. Li
School of Pharmacy, Lanzhou University, Lanzhou 730000, People's Republic of China
e-mail: yqliu@lzu.edu.cn

G. Feng
Environment and Plant Protection Institute, Chinese Academy of Tropical Agricultural Science, Danzhou 571737, People's Republic of China

L. Yang
Environmental and Municipal Engineering School, Lanzhou Jiaotong University, Lanzhou 730000, People's Republic of China

Z.-L. Liu
State Key Laboratory of Applied Organic Chemistry, Lanzhou University, Lanzhou 730000, People's Republic of China

Introduction

Brontispa longissima (Gestro) (*B. longissima*), which is mainly distributed in Southeast Asia and the Pacific Ocean islands, is a destructive pest to palm plants (Zhou *et al*., 2004; Su *et al*., 2009). Control of the *B. longissima* larvae is frequently dependent on continued applications of conventional pesticides such as organochlorine, organophosphorus, carbamate, formamidines, and pyrethroid insecticides. Although effective, their repeated use has produced risks in the development of insect resistance and residues to humans and to the environment (Luo *et al*., 2005; Xie *et al*., 2007). These problems have highlighted the need for the development of new, more ecologically acceptable methods for *B. longissima* larvae control. Accordingly, botanical antifeedants, plant-based compounds may represent new alternative strategies for selective *B. longissima* larvae control, as they are biodegradable, eco-friendly, and safe to the environment. Especially, the discovery of new antifeeding leads from plant sources, followed by using them as the useful prototypes for further modification and structure optimization, has recently been one of the important ways for the development of new antifeedants and also offered considerable promise as components of emerging integrated pest management (Garcia and Azambuja, 2004; Shaalan *et al*., 2005; Scott *et al*., 2003; Hu *et al*., 1999).

In the course of our screening for novel naturally occurring antifeedant as pest controlling agents, two naturally occurring compounds resveratrol (**1**) and combretastatin A-4 (**3a**) (Fig. 1) based on stilbene structure were found to display potential antifeedant activity against *B. longissima* in laboratory bioassays, which prompted us to use the stilbene skeletons as useful models for further optimization as antifeedants. Stilbenes are a class of naturally occurring plant polyphenols and they exhibit a wide-range of biologic activities, including pharmacological applications such as antineoplastic, antiinflammatory, antiviral, and antioxidant activities, as well as agrochemical applications spanning algicidal, fungicidal, nematicidal, insecticidal, and antifeedant activities (Shibutani *et al*., 2004; Mizuno *et al*., 2008; Creasy and Coffee, 1988; Torres *et al*., 2003; Ioset *et al*., 2001; Harmatha and Dinan, 2003; Rhoades, 1979; Feeny, 1976).

Although few stilbene analogs exhibited promising antifeeding activity, their antifeeding activity has also been evaluated against very few insects; to the best of our knowledge, however, stilbene analogs have not been previously evaluated for insecticidal activity toward *B. longissima*. In addition, systematic structure–activity relationships (SAR) have not been well determined so the chemical basis for their insecticidal properties is not yet known.

As a part of our ongoing effort to discover natural potential leads for *B. longissima* control funded by Tropical Agricultural Protection program, in this paper, we first evaluated antifeedant activities of 25 derivatives of stilbenes against *B. longissima* and studied the preliminary structure–activity relationships of these compounds. Our results revealed that the activities of different compounds varied depending on the substitution of the functional groups and the side chain attached to the olefin site of stilbenes. Present study has showed that stilbenes appear to be promising natural antifeedants and may hold potential for identification of new lead structures against *B. longissima.* In addition, to probe the relationship between the structure and the activities for the synthesized stilbene analogs, a comparative molecular field analysis (CoMFA) was also performed.

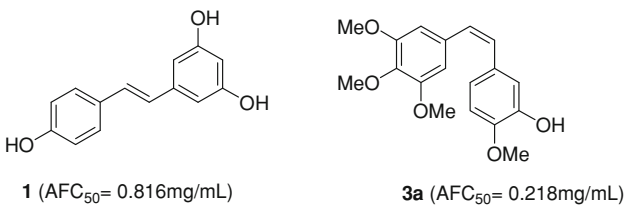

1 (AFC_{50}= 0.816mg/mL) **3a** (AFC_{50}= 0.218mg/mL)

Fig. 1 Chemical structures of stilbenes **1** and **3a**

Experimental

Chemicals

^{1}H and ^{13}C NMR spectra were measured on a Bruker AM-400 (400 MHz) spectrometer using tetramethylsilane as an internal standard (Bruker Company, USA). Mass spectra were recorded on a ZAB-HS and Bruker Daltonics APEXII49e instrument and the infrared spectra were recorded on a NIC-5DX spectrophotometer. Melting points were taken on a Kofler melting point apparatus and were uncorrected. Elemental analyses were determined on a Vario El Gmbh elemental analyzer. The synthetic compounds were purified by flash chromatography on Merck silica gel (70–230 mesh). Thin-layer chromatography (TLC) involved the use of silica gel plates with a fluorescent indicator (Merck Silica Gel 60 F_{254} 0.25 mm thick).

General procedure for preparation of compounds (**3a–s**)

A mixture of commercially available phenylacetic acids (8.84 mmol) and benzaldehydes (4.4 mmol), acetic anhydride (4 mL), and triethylamine (2 mL) were heated under reflux for 3 h. After acidification with concentrated hydrochloric acid (6 mL), the resulting solid was filtered off and recrystallised from ethanol to give acrylic acid intermediates **2a–s** as fine yellow needles. Subsequently, the corresponding acrylic acid intermediates **2a–s** (5.56 mmol) was added to powdered copper (28.8 mmol) in quinoline (20 mL) and the resulting mixture was heated at 200 °C for 2 h. Upon cooling, ether was added, and the copper was filtered off through Celite. The filtrate was washed with 1 M hydrochloric acid, and the aqueous layer was separated and extracted with ether. The combined organic layers were washed with saturated aqueous sodium carbonate, water, brine, dried ($MgSO_4$), and concentrated in vacuo. Flash column chromatography (SiO_2 petrol: EtOAc 7:3) and recrystallization from ethyl acetate and petrol afforded desired compounds **3a–s** in 30–65 % yields.

*(Z)-2-(3′-Hydroxy-4′-methoxyphenyl)-1-(3,4,5-trimethoxyphenyl) ethene (**3a**)*

Yield: 65 %; mp 117–118 °C. IR (KBr) (cm^{-1}): 3453, 3006, 1616, 1580, 1327, 1238, 1126, 1010; ^{1}H-NMR (400 MHz, $CDCl_3$) δ: 3.69 (s, 6H), 3.84 (s, 3H), 3.89 (s, 3H), 5.53 (s, 1H), 6.42 (1H, d, J = 12.4 Hz), 6.47 (1H, d, J = 12.4 Hz), 6.55 (s, 2H), 6.75 (1H, d, J = 8.3 Hz), 6.82 (1H, dd, J = 8.3, 1.9 Hz), 6.92 (1H, d, J = 1.9 Hz); ^{13}C-NMR (100 MHz, $CDCl_3$) δ: 153.07, 146.02, 145.45, 137.34, 132.93, 130.81, 129.71, 129.22, 121.32, 115.27, 110.56, 106.28, 61.15, 56.15; MS *m*/*z* (%): 316 (M^+, 100), 301 (75), 241 (8), 226 (6), 211 (5), 142 (12), 115 (8), 93

(5), 57 (8); Anal.Calc. For $C_{18}H_{20}O_5$: C, 68.40 %, H, 6.38 %. Found: C, 68.37 %, H, 6.30 %.

*(Z)-2-Phenyl-1-(3,4,5-trimethoxyphenyl) ethene (**3b**)*

Yield: 45 %; mp 106–108 °C. IR (KBr) (cm^{-1}): 2997, 2936, 1579, 1327, 1236, 1125, 1006; ^{1}H-NMR (400 MHz, $CDCl_3$) δ: 3.88 (6H, s), 3.93 (3H, s), 6.76 (2H, s), 7.04 (1H, d, $J = 12$ Hz), 7.12 (1H, d, $J = 12$ Hz), 7.28 (1 H, t, $J = 7.2$ Hz), 7.38 (2H, dd, $J = 7.6$, 2.4 Hz), 7.52 (2H, d, $J = 7.6$ Hz); ^{13}C-NMR (100 MHz, $CDCl_3$) δ: 153.37, 137.90, 137.17, 133.05, 128.68, 128.60, 128.16, 127.58, 126.40, 103.51, 60.96, 56.10; MS *m/z* (%): 270 (M^+, 100), 255 (90), 195 (25), 167 (15), 152 (15), 141 (12), 115 (8), 57 (8); Anal.Calc. For $C_{17}H_{18}O_3$: C, 75.53 %, H, 6.71 %. Found: C, 75.54 %, H, 6.72 %.

*(Z)-2-(4′-Methoxyphenyl)-1-(3,4,5-trimethoxyphenyl) ethene (**3c**)*

Yield: 71 %; mp 164–165 °C. IR (KBr) (cm^{-1}): 3002, 2938, 2836, 1610, 1579, 1508, 1459, 1419, 1328, 1182, 1025, 1004; ^{1}H-NMR (400 MHz, $CDCl_3$) δ: 3.84 (3H, s), 3.88 (3H, s), 3.93 (6H, s), 6.73 (2H, s), 6.31 (1H, d, $J = 13.6$ Hz), 6.92 (2H, d, $J = 8.8$ Hz), 6.96 (1H, d, $J = 13.6$ Hz), 7.45 (2H, d, $J = 8.8$ Hz); ^{13}C-NMR (100 MHz, $CDCl_3$) δ: 159.27, 153.36, 137.59, 133.42, 129.98, 127.73, 127.61, 126.52, 114.13, 103.24, 60.96, 56.09, 55.31; MS *m/z* (%): 300 (M^+, 100), 285 (95), 270 (5), 225 (12), 210 (5), 128 (20), 115 (8); Anal.Calc. For $C_{18}H_{20}O_4$: C, 71.98 %, H, 6.71 %. Found: C, 71.92 %, H, 6.71 %.

*(Z)-2-(4′-Hydroxyphenyl)-1-(3,4,5-trimethoxyphenyl) ethene (**3d**)*

Yield: 38 %; mp 196–198 °C. IR (KBr) (cm^{-1}): 3426, 2937, 2838, 1590, 1459, 1384,1238, 1008; ^{1}H-NMR (400 MHz, $CDCl_3$) δ: 3.88 (3H, s), 3.93 (6H, s), 4.98 (1H, s), 6.72 (2H, s), 6.92 (1H, d, $J = 11.6$ Hz), 6.84 (2H, d, $J = 8.8$ Hz), 6.95 (1H, d, $J = 11.6$ Hz), 7.42 (2H, d, $J = 8.8$ Hz); ^{13}C-NMR (100 MHz, $CDCl_3$) δ: 155.26, 153.35, 137.57, 133.40, 130.16, 127.82, 127.69, 126.57, 115.63, 103.26, 60.97, 56.09; MS *m/z* (%): 286 (M^+, 100), 271 (95), 211 (10), 168 (12), 157 (15), 128 (20), 115 (8); Anal.Calc. For $C_{17}H_{18}O_4$: C, 71.31 %, H, 6.34 %. Found: C, 71.31 %, H, 6.32 %.

*(Z)-2-(4′-Acetoxyphenyl)-1-(3,4,5-trimethoxyphenyl) ethene (**3e**)*

Yield: 56 %; mp 83–85 °C. IR (KBr) (cm^{-1}): 3006, 1750, 1620, 1580, 1327, 1237, 1126, 1012; ^{1}H-NMR (400 MHz, $CDCl_3$) δ: 2.32 (3H, s), 3.88 (3H, s), 3.93 (6H, s), 6.74 (2H, s), 6.92 (1H, d, $J = 12$ Hz), 7.09 (2H, d, $J = 8.8$ Hz), 6.99 (1H, d, $J = 12$ Hz), 7.51 (2H, d, $J = 8.8$ Hz); ^{13}C-NMR (100 MHz, $CDCl_3$) δ: 169.46, 153.37, 149.98, 137.97, 134.99, 132.86, 128.84, 127.29, 127.10, 121.79, 103.51, 60.94, 56.09, 21.12; MS *m/z* (%): 328 (M^+, 85), 286 (95), 271 (100), 211 (12), 157 (15), 128 (20), 115 (10); Anal.Calc. For $C_{19}H_{20}O_5$: C, 69.50 %, H, 6.14 %. Found: C, 69.52 %, H, 6.14 %.

*(Z)-2-(4′-Nitrophenyl)-1-(3,4,5-trimethoxyphenyl) ethene (**3f**)*

Yield: 38 %; mp 210–212 °C. IR (KBr) (cm^{-1}): 1610, 1595, 1580, 1530, 1350, 1280, 1220; ^{1}H-NMR (400 MHz, $CDCl_3$) δ: 3.90 (3H, s), 3.94 (6H, s), 6.78 (2H, s), 7.05 (1H, d, $J = 12$ Hz), 7.22 (1H, d, $J = 12$ Hz), 7.63 (2H, d, $J = 8$ Hz), 8.22 (2H, d, $J = 8$ Hz); ^{13}C-NMR (100 MHz, $CDCl_3$) δ: 153.51, 146.68, 143.75, 133.25, 131.82, 126.72, 125.67, 124.17, 104.14, 60.99, 56.17; MS *m/z* (%): 315 (M^+, 85), 300 (85), 285 (5), 211 (12), 168 (20), 152 (25), 139 (30); Anal.Calc. For $C_{17}H_{17}NO_5$: C, 64.75 %, H, 5.43 %.N, 4.44 %. Found: C, 64.75 %, H, 5.42 %, N, 4.44 %.

*(Z)-2-(4′-Chlorophenyl)-1-(3,4,5-trimethoxyphenyl) ethene (**3g**)*

Yield: 46 %; mp 153–155 °C. IR (KBr) (cm^{-1}): 3058, 3024, 2926, 2854, 1564, 1494, 1472, 1446, 1473, 1051; ^{1}H-NMR (400 MHz, $CDCl_3$) δ: 3.88 (3H, s), 3.93 (6H, s), 6.74 (2H, s), 6.98 (1H, d, $J = 12.4$ Hz), 7.04 (1H, d, $J = 12.4$ Hz), 7.33 (2H, d, $J = 8.4$ Hz), 7.44 (2H, d, $J = 8.4$ Hz); ^{13}C-NMR (100 MHz, $CDCl_3$) δ: 153.42, 138.12,135.70, 133.12, 132.70, 129.23, 128.85, 127.54, 126.83, 103.59, 60.96, 56.11; MS *m/z* (%): 304 (M^+, 85), 289 (85), 229 (8), 165 (12), 152 (25), 139 (30); Anal.Calc. For $C_{17}H_{17}ClO_3$: C 67.00 %, H 5.62 %, Cl, 11.63 %. Found: C 67.01 %, H 5.62 %, Cl, 11.66 %.

*(Z)-2-(4′,6′-Dinitrophenyl)-1-(3,4,5-trimethoxyphenyl) ethene (**3h**)*

Yield: 42 %; mp 180–181 °C. IR (KBr) (cm^{-1}): 3418, 3173, 2912, 1679, 1528, 1351, 1279, 1126; ^{1}H-NMR (400 MHz, $CDCl_3$) δ: 3.92 (3H, s), 3.94 (6H, s), 6.97 (2H, s), 7.72 (1H, d, $J = 12.4$ Hz), 7.75 (1H, d, $J = 12.4$ Hz), 7.33 (2H, d, $J = 2$ Hz), 8.22 (1H, d, $J = 2$ Hz), 9.12 (1H, s); ^{13}C-NMR (100 MHz, $CDCl_3$) δ: 159.10, 153.25, 152.74, 148.69, 139.67, 137.02, 131.40, 128.97, 128.55, 124.47, 119.28, 112.14, 106.11, 60.96, 56.33; MS *m/z* (%): 360 (M^+, 100), 342 (30), 314 (30), 197 (12), 182 (25), 126

(30); Anal.Calc. For $C_{17}H_{16}N_2O_7$: C, 56.67 %, H, 4.48 %, N, 7.77 %, Found: C, 56.65 %, H, 4.48 %, N, 7.78 %.

*(Z)-2-(4′,6′-Dichlorophenyl)-1-(3,4,5-trimethoxyphenyl) ethene (**3i**)*

Yield: 47 %; mp 117–119 °C. IR (KBr) (cm^{-1}): 3059, 2912, 1681, 1565, 1508, 1278, 1237, 1129; ^{1}H-NMR (400 MHz, $CDCl_3$) δ: 3.89 (3H, s), 3.93 (6H, s), 6.76 (2H, s), 7.01 (1H, d, $J = 12.4$ Hz), 7.24 (1H, d, $J = 12.4$ Hz), 7.26 (2H, d, $J = 2$ Hz), 7.42 (1H, d, $J = 2$ Hz), 7.61 (1H, s); ^{13}C-NMR (100 MHz, $CDCl_3$) δ: 153.43, 138.50, 133.94, 133.71, 133.37, 132.44, 131.74, 129.53, 127.29, 127.10, 123.06, 103.95, 60.96, 56.14; MS *m/z* (%): 338 (M^+, 100), 323 (30), 288 (30), 272 (40), 202 (25), 139 (30); Anal.Calc. For $C_{17}H_{16}Cl_2O_3$: C, 60.19, H, 4.75 %, Cl, 20.90 %, Found: C, 60.20 %, H, 4.76 %, Cl, 20.89 %.

*(Z)-2-(4′,5′-Diacetoxyphenyl)-1-(3,4,5-trimethoxyphenyl) ethene (**3j**)*

Yield: 47 %; mp 141–143 °C. IR (KBr) (cm^{-1}): 3002, 2954, 1705, 1584, 1510,1421, 1249, 1129, 1037; ^{1}H-NMR (400 MHz, $CDCl_3$) δ: 2.40 (6H, s), 3.87 (3H, s), 3.92 (6H, s), 6.71 (2H, s), 6.90 (1H, d, $J = 12$ Hz), 6.91 (1H, d, $J = 12$ Hz), 6.99 (1H, dd, $J = 8$ Hz), 7.01 (1H, d, $J = 8$ Hz), 7.30 (1H, s); ^{13}C-NMR (100 MHz, $CDCl_3$) δ: 153.38, 146.36, 138.77, 127.74, 126.93, 125.22, 120.06, 117.95, 103.39, 60.96, 56.10, 21.05; MS *m/z* (%): 386 (M^+, 20), 344 (60), 302 (90), 287 (100), 242 (25), 115 (30); Anal.Calc. For $C_{21}H_{22}O_7$: C, 65.28 %, H, 5.74 %. Found: C, 65.30 %, H, 5.74 %.

*(Z)-2-(4′,5′-Methylenedioxyphenyl)-1-(3,4,5-trimethoxyphenyl)ethene (**3k**)*

Yield: 73 %; mp 79–81 °C. IR (KBr) (cm^{-1}): 3006, 1620, 1582, 1327, 1238, 1126, 1010, 930; ^{1}H-NMR (400 MHz, $CDCl_3$) δ: 3.72 (6H, s), 3.85 (3H, s), 5.92 (2H, s), 6.45 (1H, d, $J = 12.4$ Hz), 6.50 (1H, d, $J = 12.4$ Hz), 6.52 (2H, s), 6.74 (1H, d, $J = 8$ Hz), 6.79 (1H, s), 6.82 (1H, d, $J = 8$ Hz); ^{13}C-NMR (100 MHz, $CDCl_3$) δ: 152.91, 147.34, 146.59, 137.17, 132.54, 131.16, 129.47, 129.13, 122.91, 109.07, 108.14, 105.98, 100.91, 60.91, 55.92; MS *m/z* (%): 314 (M^+, 100), 299 (85), 339 (30), 155 (20), 127 (25); Anal.Calc. For $C_{18}H_{18}O_5$: C, 68.78 %, H, 5.77 %. Found: C, 68.78 %, H, 5.76 %.

*(Z)-2-Phenyl-1-(4-hydroxyphenyl) ethene (**3l**)*

Yield: 42 %; mp 197–199 °C. IR (KBr) (cm^{-1}): 3430, 3002, 1585, 1520, 1510, 1250; ^{1}H-NMR (400 MHz, $CDCl_3$) δ: 5.40 (1H, s), 6.76 (1H, d, $J = 12.6$ Hz), 7.81 (1H, d, $J = 12.6$ Hz), 7.02—7.55 (m, 9H); ^{13}C-NMR (100 MHz, $CDCl_3$) δ: 155.39, 149.93, 137.58, 130.25, 129.89, 128.79, 128.63, 128.13, 127.91, 127.22, 126.85, 126.61, 126.23, 121.17, 115.63; MS *m/z* (%): 196 (M^+, 100), 181 (40), 165 (50), 152 (20), 115 (25); Anal.Calc. For $C_{14}H_{12}O$: C, 85.68 %, H, 6.16 %. Found: C, 85.68 %, H, 6.16 %.

*(Z)-2-(4′-Acetoxyphenyl)-1-(4-methoxyphenyl) ethene (**3m**)*

Yield: 47 %; mp 166–168 °C. IR (KBr) (cm^{-1}): 3006, 1745, 1620, 1585, 1326, 1237, 1126, 1005; ^{1}H-NMR (400 MHz, $CDCl_3$) δ: 2.32 (3H, s), 3.84 (3H, s), 6.91 (2H, d, $J = 8.8$ Hz), 6.98 (1H, d, $J = 11.2$ Hz), 7.01 (1H, d, $J = 11.2$ Hz), 7.08 (1H, d, $J = 8.4$ Hz), 7.45 (2H, d, $J = 8.8$ Hz), 7.49 (2H, d, $J = 8.4$ Hz); ^{13}C-NMR (100 MHz, $CDCl_3$) δ: 149.74, 128.47, 127.72, 127.12, 125.59, 121.73, 114.15, 55.33, 21.15; MS *m/z* (%): 268 (M^+, 20), 226 (100), 311 (40), 165 (30), 113 (25); Anal.Calc. For $C_{17}H_{16}O_3$: C,76.10 %, H, 6.01 %. Found: C, 76.10 %, H, 6.00 %.

*(Z)-2-(4′-Chlorophenyl)-1-(4-hydroxyphenyl) ethene (**3n**)*

Yield: 47 %; mp 181–183 °C. IR (KBr) (cm^{-1}): 3400, 1610, 1595, 1580, 1530, 1350, 1280, 1220; ^{1}H-NMR (400 MHz, $CDCl_3$) δ: 4.85 (1H, s), 6.85 (1H, d, $J = 12.6$ Hz), 6.89 (1H, d, $J = 12.6$ Hz), 6.99—7.54 (m, 8H); ^{13}C-NMR (100 MHz, $CDCl_3$) δ: 155.37, 136.09, 132.73, 130.03, 128.78, 128.71, 127.98, 127.48, 127.39, 125.35, 115.65; MS *m/z* (%): 230 (M^+, 100), 215 (20), 194 (40), 165 (30), 115 (25); Anal.Calc. For $C_{14}H_{11}ClO$: C, 72.89 %, H, 4.81 %, Cl, 15.37 %. Found: C, 72.88 %, H, 4.81 %, Cl, 15.37 %.

*(Z)-2-(4′-Nitrophenyl)-1-(4-hydroxyphenyl) ethene (**3o**)*

Yield: 36 %; mp 202–204 °C. IR (KBr) (cm^{-1}): 3420, 1610, 1592, 1580, 1530, 1350, 1280, 1220; ^{1}H-NMR (400 MHz, $CDCl_3$) δ: 5.32 (1H, s), 6.88 (2H, d, $J = 8.4$ Hz), 6.99 (1H, d, $J = 12.2$ Hz), 7.21 (1H, d, $J = 12.2$ Hz), 7.46 (2H, d, $J = 8.4$ Hz), 7.60 (2H, d, $J = 8.8$ Hz), 8.21 (2H, d, $J = 8.8$ Hz); ^{13}C-NMR (400 MHz, $CDCl_3$) δ: 147.74, 132.82, 128.64, 126.52, 124.16, 115.88; MS *m/z* (%): 271 (M^+, 100), 256 (20), 194 (30), 165 (25), 152 (20); Anal.Calc. For $C_{14}H_{11}NO_3$: C, 69.70 %, H, 4.60 %, N, 5.81 %. Found: C, 69.71 %, H, 4.60 %, N, 5.82 %.

*(Z)-2-(4′-Methoxy-5′-nitrophenyl)-1-(4-hydroxyphenyl) ethene (**3p**)*

Yield: 35 %; mp 149–151 °C. IR (KBr) (cm^{-1}): 3453, 3004, 1616, 1586, 1327, 1238, 1123, 1010; ^{1}H-NMR (400 MHz, $CDCl_3$) δ: 3.99 (3H, s), 4.85 (1H, s), 6.88 (2H,

d, $J = 8.4$ Hz), 6.91 (1H, d, $J = 12.4$ Hz), 7.02 (1H, d, $J = 12.4$ Hz), 6.85 (2H, d, $J = 4.8$ Hz), 7.07 (1H, d, $J = 8.8$ Hz), 7.40 (2H, d, $J = 4.8$ Hz), 6.82 (1H, dd, $J = 8.8$, 2.4 Hz), 7.98 (1H, d, $J = 2.4$ Hz); ^{13}C-NMR (100 MHz, $CDCl_3$) δ: 155.55, 151.89, 131.63, 130.70, 129.68, 129.04, 128.01, 123.68, 122.91, 115.72, 113.76, 56.66; MS *m/z* (%): 271 (M^+, 100), 256 (20), 194 (30), 165 (25), 152 (20); Anal.Calc. For $C_{15}H_{13}NO_4$: C, 66.41 %, H, 4.83 %, N, 5.16 %. Found: C, 66.40 %, H, 4.83 %, N, 5.18 %.

*(Z)-2-(4′-Methoxy-5′-acetoxyphenyl)-1-(4-acetoxyphenyl) ethene (**3q**)*

Yield: 58 %; mp 151–153 °C. IR (KBr) (cm^{-1}): 3006, 1734, 1616, 1578, 1327, 1236, 1126, 1010; ^{1}H-NMR (400 MHz, $CDCl_3$) δ: 2.32 (3H, s), 2.34 (3H, s), 3.92 (3H, s), 6.83 (1H, d, $J = 12.4$ Hz), 6.86 (1H, d, $J = 8.8$ Hz), 6.96 (1H, d, $J = 12.4$ Hz), 6.99 (1H, dd, $J = 8.8$, 2 Hz), 7.15 (2H, d, $J = 2$ Hz), 7.24 (1H, d, $J = 2$ Hz), 7.31 (2H, d, $J = 2$ Hz); ^{13}C-NMR (100 MHz, $CDCl_3$) δ: 169.05, 156.30, 138.70, 130.70, 128.53, 127.69, 127.24, 127.20, 126.12, 125.46, 121.77, 121.72, 120.37, 119.29, 112.41, 111.79, 110.65, 56.01, 21.15; MS *m/z* (%): 326 (M^+, 20), 284 (50), 242 (100), 227 (30), 181 (20); Anal.Calc. For $C_{19}H_{18}O_5$: C, 69.93 %, H, 5.56 %. Found: C, 69.92 %, H, 5.54 %.

*(Z)-2-(4′,5′-Diacetoxyphenyl)-1-(4-acetoxyphenyl) ethene (**3r**)*

Yield: 47 %; mp 163–165 °C. IR (KBr) (cm^{-1}): 3012, 1750, 1625, 1580, 1327, 1238, 1126, 1010; ^{1}H-NMR (400 MHz, $CDCl_3$) δ: 2.31–2.33 (9H, s), 7.01 (1H, d, $J = 12.4$ Hz), 7.12 (1H, dd, $J = 8.4$, 2 Hz), 7.17 (1H, d, $J = 12.4$ Hz), 7.34 (1H, d, $J = 2$ Hz), 7.37 (1H, s), 7.18 (2H, d, $J = 8.4$ Hz), 7.31 (2H, d, $J = 8.4$ Hz); ^{13}C-NMR (100 MHz, $CDCl_3$) δ: 169.43, 168.31, 150.26, 142.29, 136.27, 134.67, 127.54, 127.16, 124.75, 121.86, 20.64; MS *m/z* (%): 354 (M^+, 30), 312 (50), 283 (15), 270 (100), 228 (50); Anal.Calc. For $C_{20}H_{18}O_6$: C, 67.79 %, H, 5.12 %. Found: C, 67.80 %, H, 5.14 %.

*(Z)-2-(4′,5′-Methylenedioxyphenyl)-1-(4-hydroxyphenyl) ethene (**3s**)*

Yield: 62 %; mp 185–188 °C. IR (KBr) (cm^{-1}): 3453, 3000, 1620, 1580, 1327, 1242, 1126, 1010, 932; ^{1}H-NMR (400 MHz, $CDCl_3$) δ: 4.82 (1H, s), 5.98 (2H, s), 6.78 (1H, d, $J = 12.2$ Hz), 6.91 (2H, d, $J = 8.4$ Hz), 6.93 (1H, d, $J = 12.2$ Hz), 7.38 (2H, d, $J = 8.4$ Hz), 7.05 (1H, dd, $J = 8$, 2 Hz), 6.83 (1H, d, $J = 2$ Hz), 6.90 (1H, s); ^{13}C-NMR (100 MHz, $CDCl_3$) δ: 154.97, 148.09, 147.0, 132.14, 130.46, 127.69, 126.46, 126.40, 121.05, 115.55, 108.39, 105.38, 105.33, 101.06; MS *m/z* (%): 240 (M^+, 100), 181 (40), 152 (40); Anal.Calc. For $C_{15}H_{12}O_3$: C, 74.99 %, H, 5.03 %. Found: C, 74.97 %, H, 5.04 %.

(*E*)-2-(3′-Hydroxy-4′-methoxyphenyl)-1-(3,4,5-trimethoxyphenyl) ethene (**4**)

To a solution of *cis*-stilbene **3a** (0.63 mmol) in chloroform (10 mL) iodine (16 mg, 0.06 mmol, 10 mol%) was added. The resulting solution was stirred at room temperature for 30 min, after which the solution was washed thoroughly with saturated aqueous sodium metabisulfite to destroy the remaining iodine. The yellow solution was washed with water, dried ($MgSO_4$), and concentrated in vacuo to give **4**. Yield: 92 %; mp 102–104 °C. IR (KBr) (cm^{-1}): 3446, 3000, 1620, 1580, 1327, 1238, 1126, 1010; ^{1}H-NMR (400 MHz, $CDCl_3$) δ: 3.87 (s, 3H), 3.92 (s, 9H), 5.63 (s, 1H), 6.73 (s, 2H), 6.86 (1H, d, $J = 8.3$ Hz), 6.89 (1H, d, $J = 16.2$ Hz), 6.95 (1H, d, $J = 16.2$ Hz), 6.99 (1H, dd, $J = 8.3$, 1.9 Hz), 7.16 (1H, d, $J = 1.9$ Hz); ^{13}C-NMR (100 MHz, $CDCl_3$) δ: 153.34, 146.38, 145.77, 137.64, 133.29, 130.96, 127.79, 127.03, 119.17, 111.71, 111.66, 110.62, 103.34, 103.28, 60.98, 60.90, 56.13, 56.04, 55.93; MS *m/z* (%): 316 (M + , 100), 301 (75), 241 (8), 226 (6), 211 (5), 115 (8), 93 (15), 57 (20); Anal.Calc. For $C_{18}H_{20}O_5$: C, 68.34 %, H, 6.37 %. Found: C, 68.35 %, H, 6.37 %.

(*E*)-Methyl-3-(3′-hydroxy-4′-methoxyphenyl)-2-(3,4,5-Trimethoxyphenyl) prop-2-enoate (**5**)

Concentrated H_2SO_4 (2 mL) was added to a stirred solution of propenoic acid **2a** (5.35 mmol) in methanol (20 mL) and the mixture was heated under reflux overnight. Upon cooling, the solid was filtered off and recrystallised from methanol to give the ester **5**. Yield: 68 %; m.p. 177–179 °C. IR (KBr) (cm^{-1}): 3450, 3006, 1752, 1628, 1580, 1327, 1238, 1126, 1010; ^{1}H-NMR (400 MHz, $CDCl_3$) δ: 3.68 (6H, s), 3.69 (3H, s), 3.72 (3H, s), 3.74 (3H, s), 6.47 (2H, s), 6.54 (1H, d, $J = 1.9$ Hz), 6.63 (1H, dd, $J = 8.3$, 1.9 Hz), 6.82 (1H, d, $J = 8.3$ Hz), 7.61 (1H, s), 8.98 (1H, s); ^{13}C-NMR (100 MHz, $CDCl_3$) δ: 168.43, 153.55, 147.50, 145.07, 140.28, 137.69, 131.39, 130.24, 127.84, 123.75, 116.66, 110.13, 106.68, 56.15, 56.08, 55.89; MS *m/z* (%): 374 (M^+, 100), 359 (40), 315 (40),241(20), 115 (8), 59 (40); Anal.Calc. For $C_{20}H_{22}O_7$: C, 64.16 %, H, 5.92 %. Found: C, 63.98 %, H, 6.00 %.

(*E*)-3-(3′-Hydroxy-4′-methoxyphenyl)-2-(3,4,5-Trimethoxyphenyl)prop-2-en-1-ol (**6**)

To a solution of lithium aluminum hydride (39.5 mmol) in dry THF (30 mL) at –15 °C under Ar a warm saturated THF solution of ester **5** (10.7 mmol) was added dropwise.

After stirring at room temperature for 2 h, aqueous THF (5–50 % water) was added carefully until excess lithium aluminum hydride had reacted. The lithium salts were filtered off and the filtrate concentrated *in vacuo*. The aqueous layer was separated and extracted with EtOAc (3 × 50 mL). The combined organic layers were washed with water (2 × 50 mL), brine (50 mL), dried ($MgSO_4$), and concentrated *in vacuo*. Recrystallisation from EtOAc gave the alcohol **6**. Yield: 80 %; m.p. 119–120 °C. IR (KBr) (cm^{-1}): 3452, 3068, 2942, 1676, 1584, 1510, 1411, 1257, 1238, 1222, 1126, 1035; ^{1}H-NMR (400 MHz, $CDCl_3$) δ: 3.78 (6H, s), 3.85 (3H, s), 3.89 (3H, s), 4.35 (1H, d, $J = 5.7$ Hz), 5.47 (1H, s), 6.49 (2 H, s), 6.55 (1H, dd, $J = 8.3$, 1.9 Hz), 6.56 (1H, s), 6.65 (1H, d, $J = 8.3$ Hz), 6.98 (1H, d, $J = 1.9$ Hz), 7.28 (1H, s); ^{13}C-NMR (100 MHz, $CDCl_3$) δ: 153.56, 145.65, 144.95, 139.66, 137.42, 133.99, 129.75, 126.58, 126.52, 121.36, 115.32, 115.25, 110.11, 105.73, 105.66, 68.85, 56.14, 56.04; MS *m*/*z* (%): 346 (M^+, 20), 317 (5), 287 (40), 217 (20), 149 (50), 129 (60); Anal.Calc. For $C_{19}H_{22}O_6$: C, 65.88 %; H, 6.40 %. Found: C, 65.55 %, H, 6.44 %.

(*E*)-3-(3′-Hydroxy-4′-methoxyphenyl)-2-(3,4,5-trimethoxyphenyl)acrylamide (**7**)

To a solution of **2a** (1.82 mmol) in CH_2Cl_2 (9 mL) $SOCl_2$ (0.70 mL) was added in DMF (1 mL). The solution was stirred at room temperature for 1 h and then the mixture was evaporated to dryness. The residue was dissolved with CH_2Cl_2 (5 mL) and the solution was added to well-stirred 28 % aqueous NH_3 (30 mL) at room temperature. After 30 min, the reaction mixture was extracted with CH_2Cl_2 and dried over Na_2SO_4. After concentration, the residue was purified by preparative TLC (EtOAc/hexane) to give **7**. Yield: 38 %; m.p. 183–185 °C. IR (KBr): 3471, 3347, 3179, 2935, 1663, 1582, 1514, 1463, 1412, 1280, 1237, 1126, 1030, 1104; ^{1}H-NMR (400 MHz, $CDCl_3$) δ: 3.82 (s, 6H), 3.86 (s, 3H), 3.93 (s, 3H), 5.50 (s, 1H), 5.54 (bs, 2H), 6.51 (s, 2H), 6.64 (bs, 1H), 6.65 (1H, dd, $J = 2$, 8 Hz), 6.69 (1H, d, $J = 8$ Hz), 7.75 (s, 1H); ^{13}C-NMR (100 MHz, $CDCl_3$) δ: 154.26, 147.39, 145.12, 137.83, 131.90, 127.98, 123.78, 116.32, 110.18, 106.34, 61.09, 56.25, 55.84; MS *m*/*z* (%): 269 (M^+, 40), 241 (25), 165 (40); Anal.Calc. For $C_{19}H_{21}NO_6$: C, 63.50, H, 5.89, N, 3.90 %. Found: C, 56.28, H, 5.70, N, 3.45 %.

(*E*)-3-(‘4-Methoxy-3′-hydroxyphenyl)-2-(3,4,5-trimethoxyphenyl)acrylonitrile (**8**)

To a solution of **7** (0.3 mmol) in pyridine (5 mL) $SOCl_2$ (0.10 mL) was added. The reaction mixture was stirred at room temperature for 6 h. The mixture was concentrated to dryness and the residue was purified by preparative TLC (EtOAc/hexane) to give **8**. Yield: 52 %; m.p. 194–196 °C. IR (KBr) (cm^{-1}): 3346, 3186, 2934, 1661, 1581, 1508, 1459, 1410, 1275, 1237, 1125, 1024; ^{1}H-NMR (400 MHz, $CDCl_3$) δ: 3.97 (3H, s), 3.88 (3H, s), 3.78 (6H, s), 5.56 (1H, s), 6.62 (2H, s), 6.78 (1H, d, $J = 8.7$ Hz), 6.83 (1H, s), 7.29 (1H, dd, $J = 2.4$, 8.7 Hz), 7.49 (1H, d, $J = 2.4$ Hz); ^{13}C-NMR (100 MHz, $CDCl_3$) δ: 153.64, 148.02, 145.30, 143.58, 138.74, 128.01, 126.85, 123.27, 120.51, 115.62, 111.95, 110.22, 105.96, 103.22, 61.00, 56.30, 56.19, 55.94; MS *m*/*z* (%): 341 (M^+, 100), 326 (75), 149 (40); Anal.Calc. For $C_{19}H_{19}NO_5$: C, 66.85 %, H, 5.61 %, N, 4.10 %. Found: C, 66.88 %, H, 5.65 %, N, 4.12 %.

Insects

First- or second-instar larvae of *B. longissima* were collected from suburban vegetable fields of Danzhou, Hainan Povince, China, and reared in our laboratory under controlled photoperiod (12:12 h light:dark) and temperature (25 (± 1) °C) and fed daily with cabbage until they reached the earlier stage of the third-instar larvae when they were used for testing.

Insect antifeedant assay

Antifeedant activities of synthesized compounds were evaluated against third-instar larvae of *B. longissima* according to previously reported method (Liu *et al*., 2008). Briefly, a leaf-dipping method was used to evaluate the activity of the test samples. Cabbage leaves were washed with 70 % double distilled alcohol and air dried for 15 min before dipping into the required amount of compounds in acetone. The leaf disk (6.5 cm) of cabbage was used for evaluating antifeedant activity of the samples against *B. longissima*. Ten leaf disks per dose were separately dipped in each test solution for 30 s. Solvents were evaporated, and the larvae were transferred individually on treated and controlled (disks treated with solvent and emulsified water only) leaf disks placed in Petri plates. Treated leaves were fed to third-instar larvae of *B. longissima*. Five replications were used per dose for the test. Experiments were maintained at 28 ± 1 °C and 65 ± 5 % relative humidity. The antifeedant activities of synthesized compounds were determined at different concentrations (0.050, 0.125, 0.250, 0.500, and 1.000 mg/mL) after 48 h of treatment. If a whole disk was consumed, food consumption was recorded as 1. If only part of a disk was consumed, the food consumption was assessed by estimating the percentage of the surface of the leaf wafer consumed. The antifeedant rate (AR) was calculated as

$$AR = (C - T) \times 100/C$$

where C is the average consumption by one larva in the control and T in the treatment. The concentration for 50 %

antifeedant effect (AFC_{50}) was determined by log-probit analysis. All data were treated by log-probit analysis and 95 % fiducial limits were calculated.

Molecular modeling and CoMFA analysis

All molecular modeling and calculation studies were performed by means of the Sybyl 6.9 programs running on an SGI Origin server. The structures were built and optimized by means of Tripos force field with a distance-dependent dielectric function until a root mean square (RMS) deviation of 0.005 kcal/mol. Next, the structures were extracted and optimized by the PM3 method. The conformational search was performed by multisearch method with the following settings: maximum cycles (400), maximum conformers (400), energy cutoff (70 kcal/mol), maximum RMS gradient (3.0) tolerance (0.40), and number of hit (12). The derived minimum energy conformation thus was used in the analysis. Alignment criteria play an important role in CoMFA studies and it is preferable to choose an alignment which maintains the bioactive conformation. In the present study, the optimized structures of 25 molecules were aligned on the template molecule '**3a**' which had the highest activity by the database alignment method.

CoMFA steric and electrostatic interaction fields were calculated at each lattice intersection on a regularly spaced grid of 2.0 Å. The grid pattern was generated automatically by the Sybyl/CoMFA routine and extended 4.0 Å units in the *X*, *Y*, and *Z* directions beyond the dimensions of each molecule. A sp^3-hybridized carbon atom with a van der Waals of 1.52 Å and a +1.0 charge was used as the probe to calculate the steric field energies and electrostatic fields with a distance-dependent dielectric at each lattice point. Values of the steric and electrostatic fields were truncated to 30 kcal/mol.

Partial least squares (PLS) analysis was used to correlate the molecular fields and the activities with magnitude of steric, electrostatic, and other potentials. The optimal number of components was determined by SAMPLS (Samples-distance Partial Least Square) and cross-validation was carried out by the leave-one-out method. The final CoMFA model with an optimal number of components obtained by means of LOO cross-validation and with the highest (q^2) and with the lowest standard error considered.

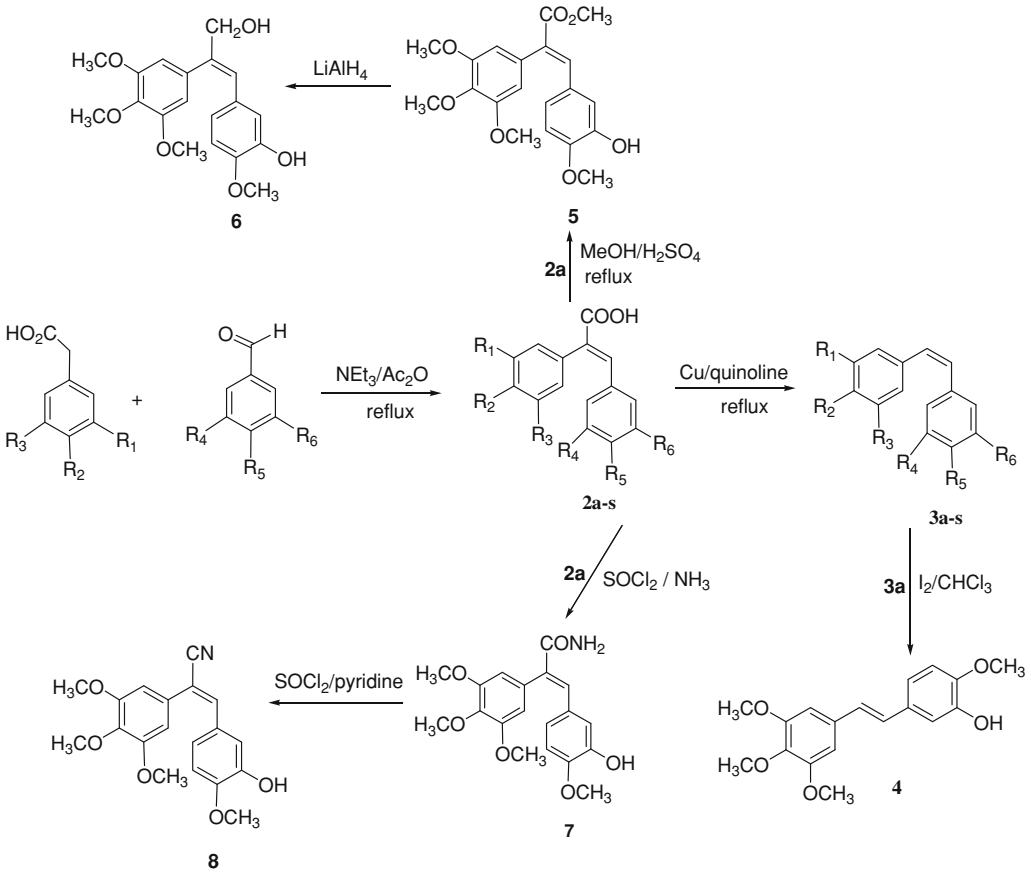

Fig. 2 Synthesis of compounds **3a–s** and **4–8**

Results and discussion

Synthesis

As shown in Fig. 2, a series of desired compounds **3a–s** were obtained via the Perkin condensation of commercially available phenylacetic acids and benzaldehydes followed by decarboxylation of the acrylic acid intermediates **2a–s** using copper and quinoline. In this reaction, only pure *cis*-isomers were obtained in moderate yields (30–65 %) after purification of the crude precipitate by fractional crystallization. The iodine-catalyzed isomerization of the representative *cis*-stilbene **3a** resulted in complete conversion to the corresponding *trans*-stilbene **4**. The *cis* and *trans* configurations of these compounds were confirmed by measuring the characteristic coupling constants of the olefinic protons in the NMR spectra. The cinnamic acid **2a** was first converted to the methyl ester **5** which was reduced with $LiAlH_4$ to afford alcohol **6**. The acid **2a** was converted to amide **7** by treatment with $SOCl_2$ followed by aqueous NH_3 treatment. The acrylamide **7** was then reacted with $SOCl_2$ to give acrylonitrile **8**.

Table 1 Antifeedant activities of stilbene derivatives against third-instar larvae of *B. longissima*

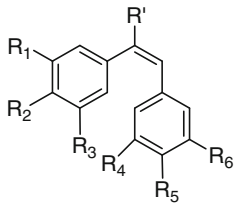

Compd.	A-ring			B-ring			AFC_{50} (mg/mL) (95 % fiducial limits)
	R_1	R_2	R_3	R_4	R_5	R_6	
3a	OCH_3	OCH_3	OCH_3	H	OCH_3	OH	0.218 (0.137–0.274)
3b	OCH_3	OCH_3	OCH_3	H	H	H	0.529 (0.372–0.663)
3c	OCH_3	OCH_3	OCH_3	H	OCH_3	H	0.327 (0.243–0.410)
3d	OCH_3	OCH_3	OCH_3	H	OH	H	1.261 (0.864–1.580)
3e	OCH_3	OCH_3	OCH_3	H	OAc	H	0.843 (0.629–1.057)
3f	OCH_3	OCH_3	OCH_3	H	NO_2	H	0.982 (0.585–1.231)
3g	OCH_3	OCH_3	OCH_3	H	Cl	H	1.634 (1.018–2.048)
3h	OCH_3	OCH_3	OCH_3	NO_2	H	NO_2	1.05 (0.698–1.316)
3i	OCH_3	OCH_3	OCH_3	Cl	H	Cl	2.234 (1.567–2.799)
3j	OCH_3	OCH_3	OCH_3	H	OAc	OAc	1.918 (1.334–2.404)
3k	OCH_3	OCH_3	OCH_3	H	$–OCH_2O–$		0.731 (0.533–0.916)
3l	H	OH	H	H	H	H	1.161 (0.494–1.455)
3m	H	OAc	H	H	OCH_3	H	0.732 (0.464–0.917)
3n	H	OH	H	H	Cl	H	0.412 (0.269–0.516)
3o	H	OH	H	H	NO_2	H	1.185 (0.892–1.485)
3p	H	OH	H	H	OCH_3	NO_2	1.301 (0.905–1.630)
3q	H	OAc	H	H	OCH_3	OAc	2.501 (1.528–3.134)
3r	H	OAc	H	H	OAc	OAc	0.64 (0.450–0.803)
3s	H	OH	H	H	$–OCH_2O–$		1.005 (0.471–1.259)
4							0.357 (0.260–0.447)
5							1.453 (0.890–1.821)
6							0.226 (0.108–0.284)
7							0.736 (0.518–0.923)
8							0.431 (0.302–0.540)
2a							1.461 (0.994–1.830)

Biologic activity

With the 25 stilbene derivatives in hand, we next examined their antifeedant effects against third-instar larvae of *B. longissima*. The results were summarized in Table 1. In view of our goal to contribute to robust SAR studies and develop potential insect antifeedants, many modifications, related to chemical features of the molecule (i.e., double bond geometry and substitution pattern of both rings), were evaluated in detail. First, for the compounds with 3,4,5-trimethoxy group on the A-ring, these analogs with different substituents on the B-ring seemed to be preferred for antifeedant activities. Among the test compounds, **3a**–**3c** possessed the highest overall antifeedant potency with AFC_{50} values of 0.218, 0.529, and 0.327 mg/mL against third-instar larvae of *B. longissima*, respectively.

The small differences in activities observed between **3a** and **3c** could only be attributed to the extra OH in the structure of **3a**, which seemed slightly to increase the antifeedant activity. In comparing the antifeedant effects at the 4′-position of the B-phenyl ring, compounds with electron-donating methoxy group were generally more potent than those with the electron-withdrawing nitro or chloro moieties. For example, replacement of 4-OMe of the B-ring with a 4-NO_2 group (**3f**) or 4-OAc group (**3e**) resulted in approximately threefold decrease in antifeedant potency. A further dramatic loss of activity was observed by replacement of 4-OMe of the B-ring with a 4-chloro group (**3g**), as Table 1 showed. In comparison with **3c**, introduction of a hydroxy group (**3d**) on the B-ring severely weakened the antifeedant potency. Similarly, those bearing two chloro or nitro groups on the 3′, 4′-position of the B-ring (**3h** and **3i**) also showed a five- to tenfold decreased antifeedant effects. The results also clearly underlined the antifeedant differences could be ascribed to a combination of factors, like the nature of the substitutes (which may depend on the size of substitutes, electronic characteristics of substitutes, or other factors) or a different interaction at the site. Next, we turned our attention to variations in other parts of the hydroxy or acetyl groups at the 4-position of the A-ring (**3l**–**s**); a similar trend could be observed for variations of the 3,4,5-trimethoxy group on the A-ring where only few minor structural changes were tolerated. Unexpectedly, compound **3n** was found to be the most active (AFC_{50}, 0.412 mg/mL) and it was 4-times more potent than **3g** (AFC_{50}, 1.634 mg/mL).

Subsequently, in an effort to better understand the structure–activity relationships of this class of derivatives, we examined small substituents on the olefin site (**2a** and **5**–**8**). As shown in Table 1, compounds **2a** and **5** displayed approximately sevenfold decreased activity comparable to natural **3a** although they still remained antifeedant activity. Strikingly, acrylamide **7** was significantly more potent than **2a**. Introduction of a hydroxymethyl group resulted in a compound (**6**, $AFC_{50,}$ 0.226 mg/mL) which had comparable antifeedant activity than the parent compound **3a**. Also, nitrile **8** showed slightly decreased antifeedant activity ($AFC_{50,}$ 0.431 mg/mL) comparable to **3a**. These results demonstrated that the insertion of different substituents onto the olefin site adjacent to the A-ring resulted in weaker activity and a nitrile group was about the maximum tolerable size. Furthermore, the difference between *cis*- and *trans*-isomers **3a** and **4** in antifeedant activity was significant and indicated the relative importance of the spatial arrangement of the molecule in the activity displayed.

CoMFA analysis

In this study, CoMFA analysis was applied based on the 25 compounds which were divided into a training set with 20 compounds (unasterisked molecule in Table 2) for model construction and a test set with the remaining 5 compounds (asterisked molecules in Table 2) for model validation.

Table 2 Predicted activities from CoMFA models compared with the experimental activities and the residues

Compounds	Experimental $pAFC_{50}$	Predicted $pAFC_{50}$	Residual
2a	−0.17	−0.29	0.12
3a	0.66	0.67	−0.01
3b	0.28	0.28	0.00
3c	0.48	0.47	0.01
3d	−0.10	−0.18	0.08
3e	0.07	0.02	0.05
3f	0.01	0.02	−0.01
3g	−0.21	−0.19	−0.03
3h	−0.02	−0.08	0.06
3i	−0.35	0.08	−0.43
3j	−0.28	−0.25	−0.03
3k	0.14	0.08	0.05
3l	−0.06	−0.05	−0.02
3m	0.14	0.22	−0.09
3n	0.39	0.23	0.16
3o	−0.07	−0.03	−0.04
3p	−0.11	−0.12	0.00
3q	−0.40	−0.37	−0.03
3r	0.19	0.18	0.01
3s	0.00	0.09	−0.09
4	0.45	0.57	−0.12
5	−0.16	−0.05	−0.11
6	0.65	0.50	0.15
7	0.13	0.04	0.09
8	0.36	0.38	−0.02
Test set			

Table 3 Summary of CoMFA analysis

CoMFA	Result
R^2 cross-validated (q^2)	0.533
Number of components	3
Non cross-validated r^2	0.929
Standard error of estimate	0.085
Fish test	70.309
Steric contribution	0.415
Electrostatic contribution	0.585

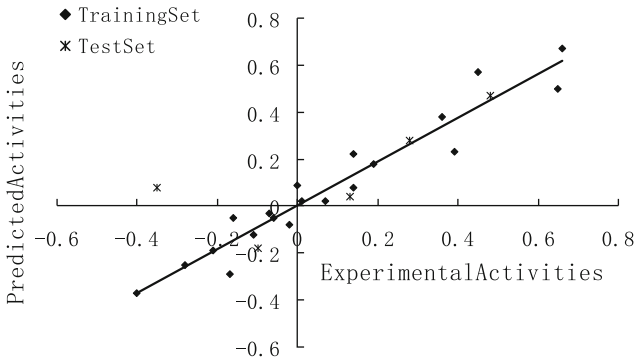

Fig. 3 Plot of observed versus predicted activity based on the CoMFA model

The activity values expressed as negative log unit of antifeedant activity ($pAFC_{50}$) were used as dependent variables. As summarized in Table 3, CoMFA analysis was carried out and the obtained PLS models yielded cross-validated q^2 value of 0.533 with 3 components. Subsequently, a non-cross validated PLS model for training set was also developed with a regression coefficients r^2 of 0.929, Fish test value of 70.309, and a standard error of estimated (SEE) of 0.107. In addition, to evaluate the predictive ability of this model, the test set was applied to verify if the development model can predict the activity of compounds that were structurally distinct from those included in the training set. As it can be seen in Table 2, the predicted activities of compounds from both training and test set were listed together with the residue. Figure 3 depicts a good correlation between the predicted activities and the experimental ones of the training and test set, which indicated that the developed CoMFA model was reliable.

For the CoMFA model, the contributions of steric and electrostatic field were 41.5 % and 58.5 %, respectively. The CoMFA contour map of steric field was shown in Fig. 4a. Considering the R_2 position, there was a large green contour below it. However, there was also yellow field close to it which indicated careful substituent group selection for this region.

With respect of R' substitute, a moderate yellow contour around the R' position indicated that the sterically bulky group was disfavored for activity in these areas. It may be the reason why compound **6** ($R' = CH_2OH$) was more active than compound **5** ($R' = CO_2CH_3$). Figure 4b showed electrostatic contour map. Considering the R_2 position; there was a large blue contour below it, but close to it there was also a moderate red contour near it, indicating careful substituent group selection for this region. There were two moderate red contours close to the R_6 position, suggesting that any negative charge or electron sufficient substitute would enhance the activity. It could well explain that the activity of compound **3h** ($R_6 = NO_2$) was higher than that of the corresponding compound **3i** ($R_6 = Cl$). A moderate blue contour was observed beside the R_5 position, revealing that positive charge was favored. For example, the activity of compound **3g** ($R_5 = Cl$) was lower than that of **3b** ($R_5 = H$).

Further investigation on the SAR was carried out by CoMFA analysis. The results demonstrated that the established 3D QSAR model was statistically reliable with good predictive power ($r^2 = 0.929$ and $q^2 = 0.533$). In addition, based on the CoMFA contours, details on the relationship between structure and the activities, as well as clues for structural modifications, were also explained. The results not only lead to a better understanding of structural requirements of antifeedant activities but also can help in the design of novel compounds with enhanced activity.

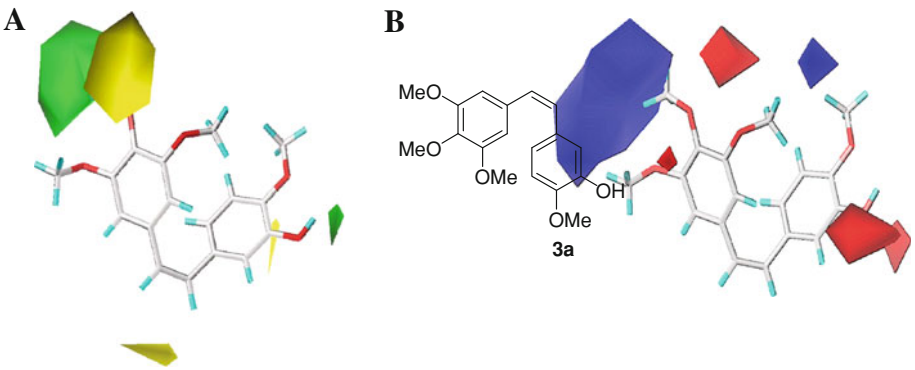

Fig. 4 Steric and electrostatic CoMFA maps of the compound **3a** (**a**). The *green* colored contour favors steric bulk while sites where steric bulk is disfavored are shown in *yellow*. **b** The *red* contour shows regions where electronegative substituents are favored, while the *blue* contour is associated with positions where electropositive substituents improve activity (Color figure online)

Conclusion

In summary, the antifeedant activities of 25 new synthetic stilbene analogs were first investigated in relation to their chemical structures. Among these analogs, compounds **3a**, **3c,** and **6** showed pronounced antifeedant activities with AFC_{50} values of 0.218, 0.327, and 0.226 mg/mL, respectively. The different antifeedant activity ranges of these compounds indicated that variation of chemical structures in the stilbene skeleton markedly affected the activity profiles of this compound class and some important SAR information was also revealed. This research has provided a new class of compounds for further investigation toward the discovery of environment-friendly antifeedants.

Acknowledgments This work was financially supported by the National Natural Science Foundation of China (30800720, 20972061); the Post-Doctor Research Foundation (20090450142); the Fundamental Research Funds for the Central Universities (lzujbky-2009-98); Key Scientific Research Programme of EPPI (2010hzsZDZX003) of Chinese Academy of Tropical Agricultural Science from the Ministry of agriculture; the Fundamental Research Funds for the Central Universities (zujbky-2010-134) and Natural Science Foundation of Gansu Province (0916RJZA033).

Conflict of interest The authors report no conflict of interest. The authors alone are responsible for the content and writing of the article.

References

Creasy LL, Coffee M (1988) Phytoalexin production potential of grape berries. J Am Soc Hortic Sci 113:230–234

Feeny PP (1976) In: Wallace JW, Mansell RL (1976) Biochemical interactions between plants and insects. Plenum Press, New York, pp 1–40

Garcia ES, Azambuja P (2004) Lignoids in insects: chemical probes for the study of ecdysis, excretion and Trypanosoma cruzi–triatomine interactions. Toxicon 44:431–440

Harmatha J, Dinan L (2003) Biological activities of lignans and stilbenoids associated with plant–insect chemical interactions. Phytochem Rev 2:321–330

Hu KJ, Li JX, Webster JM (1999) Nematicidal metabolites produced by *Photorhabdus luminescens* (Enterobacteriaceae), bacterial symbiont of entomopathogenic nematodes. Nematology 1:457–469

Ioset JR, Marston A, Gupta MP, Hostettmann K (2001) Five new prenylated stilbenes from the Root Bark of *Lonchocarpus chiricanus*. J Nat Prod 64:710–715

Liu YQ, Liu YQ, Xiao H, Gao R, Tian X (2008) Synthesis and insecticidal activities of novel derivatives of podophyllotoxin: part XII. Pest Biochem Physiol 91:116–121

Luo YP, Cai DC, Zhu ZH, Huang GD (2005) Efficacy of several insecticides against *Brontispa longissima*. Chin J Pest 44:142–143

Mizuno CS, Schrader KK, Rimando AM (2008) Algicidal activity of stilbene analogues. J Agric Food Chem 56:9140–9145

Rhoades DF (1979) In: Rosenthal GA, Janzen DH (eds) Herbivores: their interactions with secondary plant metabolites. Academic Press, New York, pp 3–54

Scott IM, Jensen H, Scott JG, Isman MB, Arnason JT, Philogène BJR (2003) Botanical insecticides for controlling agricultural pests: piperamides and the Colorado potato beetle *Leptinotarsa decemlineata* cay (Coleoptera: Chrysomelidae). Arch Insect Biochem Physiol 54:212–225

Shaalan EAS, Canyon D, Younes MWF, Abdel-Wahab H, Mansour AH (2005) A review of botanical phytochemicals with mosquitocidal potential. Environ Int 31:1149–1166

Shibutani S, Samejima M, Doi S (2004) Effects of stilbenes from bark of Picea glehnii (Sieb. et Zucc) and their related compounds against feeding behaviour of Reticulitermes speratus (Kolbe). J Wood Sci 50:439–444

Su Z, Deng LH, Yi XP, Xiao SS, Zhang CF (2009) The biocontrol of *Brontispa longissima*. Gen Appl Biol 28:405–407

Torres P, Avila JG, de Vivar AR, Garcia AM, Marin JC, Aranda E, Cespedes CL (2003) Antioxidant and insect growth regulatory activities of stilbenes and extracts from Yucca periculosa. Phytochemistry 64:463–473

Xie SH, Chen MC, Rui K, Xiao TB, Kong XY, Wu FZ (2007) The measurement of toxicity of 36 pesticides against *Brontispa Longissima*. Nat Sci J Hainan Univer 25:57–61

Zhou R, Zeng L, Liang GW, Lu YY, Cui ZX (2004) Life history of the laboratory population of the palm leaf beetle *Brontispa longiss*. Entomol Knowl 41:336–341